Evaluation of K_0 in stiff clay by back-analysis of convergence measurements from unsupported cylindrical cavity

J. Rott, D. Mašín[1], J. Boháč, M. Krupička and T. Mohyla

Charles University in Prague

Institute of Hydrogeology, Engineering Geology and Applied Geophysics

Albertov 6

12843 Prague 2, Czech Republic

E-mail: masin@natur.cuni.cz

Tel: +420-2-2195 1552, Fax: +420-2-2195 1556

April 15, 2015

Manuscript submitted to Acta Geotechnica

[1]corresponding author

1 Abstract

The coefficient of earth pressure at rest K_0 of fine-grained soils is often being estimated empirically from the overconsolidation ratio (OCR). The relationships adopted in this estimation, however, assume that K_0 is caused by pure mechanical unloading and do not consider that a significant proportion of the apparent preconsolidation pressure may be caused by the effects ageing, in particular by a secondary compression. In this work, K_0 of Brno Tegel, which is a clay of stiff to hard consistency (apparent vertical preconsolidation pressure of 1800 kPa, apparent OCR of 7), was estimated based on back-analysis of convergence measurements from unsupported cylindrical cavity. The values were subsequently verified by analysing a supported exploratory adit and a two-lane road tunnel. As the simulation results are primarily influenced by soil anisotropy, it was quantified in an experimental programme. The ratio of shear moduli α_G was 1.45, the ratio of horizontal and vertical Young moduli α_E was 1.67 and the value of Poisson ratio ν_{tp} was close to 0. The soil was described using a hypoplastic model considering small-strain stiffness anisotropy. For the given soil, the OCR-based estimation yielded $K_0 = 1.3$, while the Jáky formula estimated $K_0 = 0.63$ for the state of normal consolidation. The back-analysed value of K_0 was 0.75. The predicted tunnel displacements agreed well with the monitoring data, giving additional confidence into the selected modelling approach. It was concluded that OCR-based equations should not be used automatically for K_0 estimation. K_0 of many clays may actually be lower than often assumed.

Keywords: Stiffness anisotropy; overconsolidation; clay; tunnel; coefficient of earth pressure at rest; hypoplasticity

2 Introduction

The initial stress state represents an important ingredient of any numerical analysis of boundary value problem in geotechnical engineering. Typically, the horizontal effective stress σ_h is calculated from the known vertical effective stress σ_v using the coefficient of earth pressure at rest $K_0 = \sigma_h/\sigma_v$. As an example of the K_0 influence on boundary value problem predictions, let us cite Franzius et al. [8]. They investigated the influence of K_0 on the results of 3D finite element analyses of a tunnel in London clay. They performed two sets of analyses, one with $K_0 = 1.5$ and the other with $K_0 = 0.5$. The low K_0 value (considered as unrealistic for London clay) led to improved predictions, namely the normalized settlement trough was narrower and deeper. Similar conclusions were achieved by Doležalová [6]: decreasing the K_0 value from 1.5 to 0.5 closed up the settlement trough and increased vertical settlements in absolute terms.

Notwithstanding its importance, methods for K_0 quantification remain approximate and K_0 estimation using different methods often leads to conflicting results. Various methods of K_0 measurement have been summarised by Boháč et al. [3]. The direct methods are represented by self boring pressuremeter [36], the flat dilatometer [16] or different types of pushed-in spade-shaped pressure cells [35]. It is to be noted that although these methods are being classified as direct, empirical relationships are still needed for the data evaluation as the measurement process inevitably causes soil disturbance. Another means of direct K_0 measurement is a hydraulic fracturing technique [2, 15, 11].

Among the indirect methods of K_0 estimation, three may be considered as the most important. In the first one, negative pore water pressures are measured after the sample extraction from the ground using suction probe [31, 5, 7]. The negative pore water pressure is affected by the effective mean stress in the ground and undrained unloading stress path, which can be used to estimate K_0 based on the known *in situ* vertical effective stress. The second method, which is simple to utilise and thus often used, estimates K_0 from the preconsolidation pressure measured in oedometric compression by means of empirical correlations involving overconsolidation ratio (OCR) [23]. In the third method, K_0 is estimated on the basis of back-analyses of monitoring data from real geotechnical structures.

Let us now comment on the last two methods. The formula by Mayne and Kulhawy [23] for the estimation of K_0 from the preconsolidation pressure is based on laboratory experiments on soils subject to mechanical unloading. For stiff (apparently overconsolidated) clays it often yields values of K_0 higher than one. It is important to point out, however, that the preconsolidation measured on natural stiff clay samples may be caused not only by mechanical unloading, but also by secondary compression and other effects of ageing. Unfortunately the opinions on the influence of secondary compression on the value of K_0 [30] have not been settled satisfactorily to date. The C_α/C_c concept predicts an increase in K_0 during secondary compression of normally consolidated clays [24, 25]. The idea of "minimum energy state" with $K_0 = 1$ (i.e. stress isotropy) at geological time scale, implying an increase in K_0 for normally consolidated, and decrease in K_0 for mechanically overconsolidated clays seems plausible [14]. Due to the lack of experimental data for such large time intervals it can be just assumed that secondary compression may lead to K_0 not higher than one. Mayne and Kulhawy [23] approach to K_0 estimation is thus unreliable unless the geological history of the soil massif is precisely known. The last method, adopting back-analyses of deformations of real geotechnical structures, has also its shortcomings. In particular, it can only be used if the mechanical behaviour of the soil is accurately represented by the constitutive model, which is often not the case.

The present paper is part of a larger research project focused on estimation of K_0 in a massif of stiff to hard Tertiary clay from Brno, Czech Republic. The present work focused on K_0 quantification on the basis of back-analyses of deformation measurements of an unsupported cylindrical cavity. To eliminate ambiguity in material characterisation, advanced non-linear material model was adopted, capable of predicting small strain stiffness non-linearity and very small strain stiffness anisotropy. The structure of this paper is as follows. After introducing the problem, material model and its calibration, the back-analyses of K_0 using the monitoring data from an unsupported horizontal cylindrical cavity are presented. The models are subsequently verified by simulations of other thoroughly monitored geotechnical structures in the same soil: a large-span road tunnel and a supported exploratory adit.

3 Královo Pole tunnels and the simulated cylindrical cavity

The Královo Pole tunnels (also referred to as Dobrovského tunnels) form a part of the northern section of the ring road of Brno town in the Czech Republic. The tunnels consist of two parallel tubes with a separation distance of about 70 m[1] and lengths of approximately 1250 m. The tunnel cross-section height and width are about 12 m and 14 m respectively, and the overburden thickness varies from 6 m to 21 m. The tunnels are driven in a developed urban environment (see Fig. 1). As the tunnels and preceding exploratory adits have been thoroughly monitored, the tunnels have previously been used for validation of numerical models [34, 32, 33].

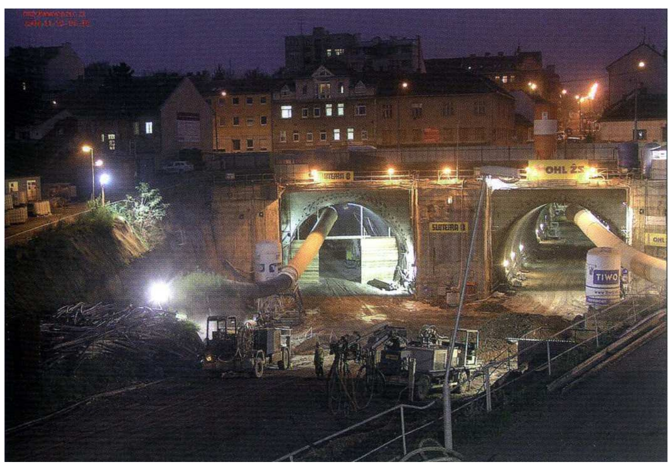

Figure 1: Temporary portals of the Královo Pole tunnels (Horák [12]).

The geological sequence in the area is shown in Fig. 2. From the stratigraphical point of view, the area is formed by Miocene marine deposits of the Carpathian fore-deep. The top part of the overburden consists of anthropogenic materials. The natural Quaternary cover consists of loess loams and clayey loams with the thickness of 3 to 10 m. The base of the Quaternary cover is formed

[1]Their distance in the portal area is 10 m and their axes are diverging, but most of their length they run parallel at an average distance of 70 m.

by a discontinuous layer of fluvial sandy gravel, often with a loamy admixture. The majority of the tunnel is driven through the Tertiary calcareous silty clay (known locally as Brno Tegel). The thickness of the clay deposit is presumed to be up to several hundreds of metres [27]. The clays are of stiff to hard consistency and high plasticity. The water table is located in the Quaternary sandy-gravel strata.

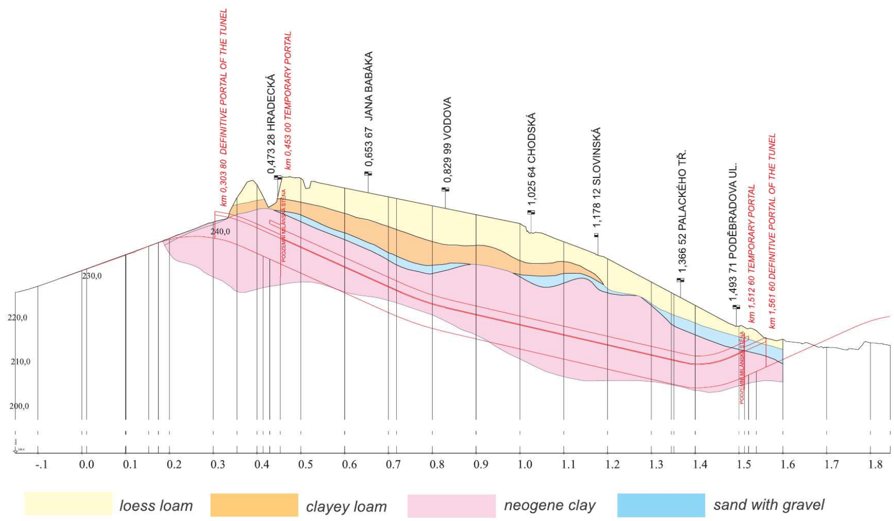

Figure 2: Longitudinal geological cross-section along the tunnels (Pavlík et al. [27]).

The Královo Pole tunnels were driven by the New Austrian Tunneling Method (NATM), with subdivision of the face into six separate headings (Fig. 3). The face subdivision, and the relatively complicated excavation sequence (Fig. 3), were adopted in order to minimise the surface settlements imposed by the tunnel [1]. The excavation was performed in steps b-a-d-c-e-f (Fig. 3) with an unsupported span of 1.2 m. A constant distance of 8 m is kept between the individual faces, except the distance between the top heading and the bottom, which was 16 m.

The inactive headings are protected by shotcrete. The unsupported length (one excavation step) is 1.2 m. The primary lining consisted of one rolled HEB steel beam per 1 m with the thickness of 240 mm, two layers of sprayed concrete of thickness of 175 mm (the overall thickness of sprayed concrete was 350 mm). The sprayed concrete layers were supplemented by steel wire meshes.

Before the Královo Pole project, there was little experience with the response of the Brno Tegel to tunnelling. In order to clarify the geological conditions of the site, and in order to study the mechanical response of the Brno Tegel, a comprehensive geotechnical site investigation programme was undertaken, the crucial part of it being an excavation of three exploratory drifts [37]. The drifts were triangular in cross section with the sides of 5 m and were designed to become parts of the top headings of the final tunnels.

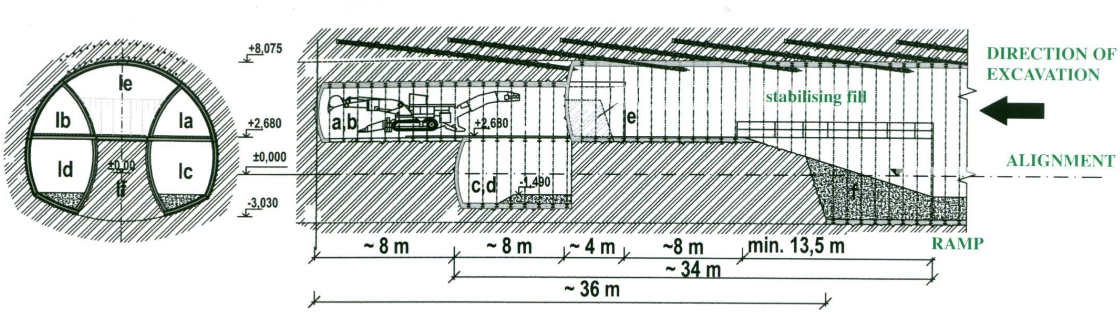

Figure 3: Sketch of the excavation sequence of the tunnel (Horák [12]).

To investigate the value of the coefficient of earth pressure at rest in Brno Tegel, four unsupported adits of circular cross-section have been excavated [27] as side-drifts from the triangular exploratory adits. The side-drift adit adopted in the present study (denoted as R2) is L-shaped (Fig. 4a). The diameter of the unsupported adit is 1.9 m; the section perpendicular to the main triangular adit is 5.4 m long. Figure 4b shows a photo from the excavation. An apparent support seen in Fig. 4b (steel arches and steel wire meshes) has been installed for safety reason only; it has not been it touch with the soil so for the purpose of the simulations the adit can be considered as unsupported. The convergence of the cylindrical cavity was measured in four profiles rotated by 45° (Fig. 5) in a section located 2.55 m from the intersection with the triangular gallery. Measurements from January 16, 2003 (as indicated in Fig. 5) were adopted in the back-analyses. This was the last measurement before the corner part of the cavity was excavated; therefore, it was sufficient to include the straight part of the cavity in the 3D numerical model. The measured values of convergences were $u_h = 19.8$ mm (convergence in the horizontal direction) and $u_v = 15.86$ mm (convergence in the vertical direction).

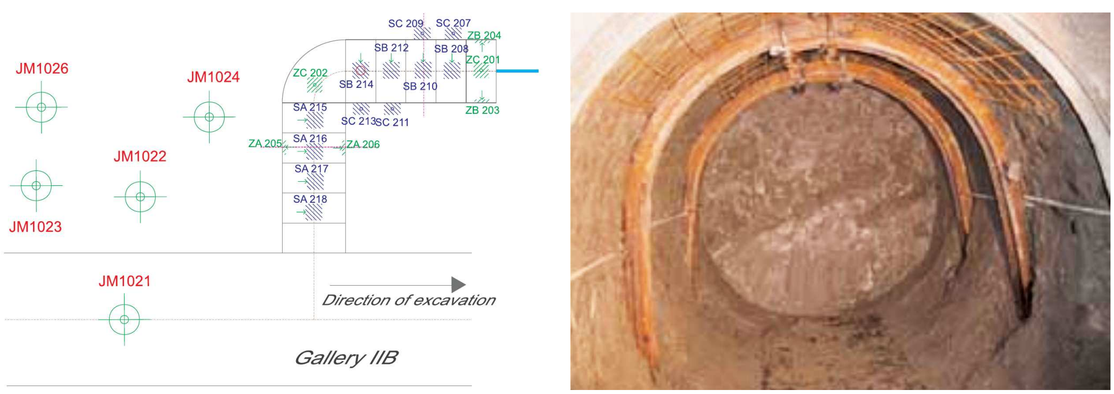

(a) (b)

Figure 4: (a) plan view of the main triangular exploratory adit "Gallery IIB" with the L-shaped cavity of circular cross-section (Pavlík et al. [27]); (b) Photo from the cylindrical cavity excavation (Pavlík et al. [27]).

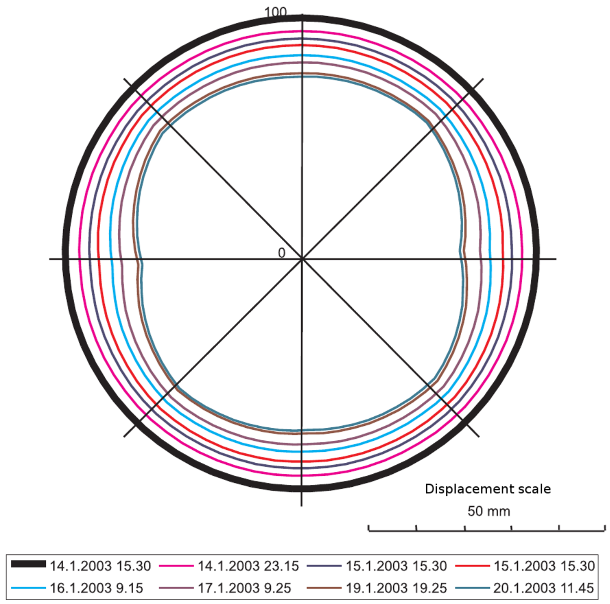

Figure 5: Convergence measurements from cylindrical cavity R2 [27].

4 Material models and their calibration

The most important aspect for the present analyses is the correct representation of the behaviour of Brno Tegel. This material has been modelled using hypoplastic model for clays incorporating very small strain stiffness non-linearity and stiffness anisotropy, developed by Mašín [21]. Part of the model parameters have been calibrated using experimental data on reconstituted and undisturbed Brno Tegel published earlier by Svoboda et al. [34]. These soil samples have been obtained during the geotechnical site investigation for the Královo pole tunnel and are thus the most representative for the present simulations.

The tests by Svoboda et al. [34], however, did not study soil stiffness anisotropy, which is one of the crucial factors influencing K_0 back-analyses. For this reason, new Brno Tegel samples have been extracted from the ground and additional tests have been performed. As the Královo pole area is not accessible any more for sample excavation, a new borehole has been drilled in a different locality (named ”Slatina”), located approximately 8.5 km from Královo pole tunnel. Thanks to the remarkable homogeneity of Brno Tegel massif, it could be assumed that the anisotropy of the new samples fairly represents the stiffness anisotropy of Brno Tegel at the Královo pole tunnel site.

4.1 Clay hypoplastic model of Brno Tegel

The hypoplastic model is based on the theory of hypoplasticity, which means it is governed by the following primary equation [9]:

$$\mathring{\mathbf{T}} = f_s \left(\boldsymbol{\mathcal{L}} : \mathbf{D} + f_d \mathbf{N} \|\mathbf{D}\| \right) \tag{1}$$

where $\mathring{\mathbf{T}}$ and $\mathbf{D}$ represent the objective (Zaremba-Jaumann) stress rate and the Euler stretching tensor respectively, $\boldsymbol{\mathcal{L}}$ and $\mathbf{N}$ are fourth- and second-order constitutive tensors, and f_s and f_d are two scalar factors. The model incorporating stiffness anisotropy [21] is an evolution of the original model for clays [17], which was reformulated to consider explicit asymptotic states [10, 18, 19, 20] and combined with the anisotropic stiffness formulation proposed in [22]. Detailed model description is outside the scope of the present paper, calibration of the most important parameters is only presented here.

The soil parameters N, λ^* and κ^* have been calibrated using oedometer tests on undisturbed samples ($\alpha_G = 1$ was considered in calibration of the basic model), see Fig. 6a. The parameters φ_c and ν have been calibrated using undrained triaxial tests on undisturbed samples (see [34] and [20]). The very small strain shear modulus G_{tp0} is in the model [21] represented using equation

$$G_{tp0} = A_g \left(\frac{p}{p_r} \right)^{n_g} \tag{2}$$

with parameters A_g and n_g. They have been quantified using the results from bender element measurements on vertically trimmed Brno Tegel samples (see Fig. 6b). The remaining parameters controlling very small strain stiffness nonlinearity (R, β_r, χ and m_{rat}) [26] have been calibrated using undrained triaxial tests on undisturbed samples with the local LVDT measurements of sample deformation [34]. The parameters are summarised in Table 1. In the finite element simulations, void ratio $e = 0.83$ and unit weight $\gamma = 18.8$ kN/m^3 were considered (following [34]).

Table 1: *Brno Tegel parameters of the hypoplastic model.*

φ_c	λ^*	κ^*	N	ν	A_g	n_g	m_{rat}	R	β_r	χ
22°	0.128	0.015	1.51	0.33	5300	0.5	0.5	0.0001	0.2	0.8

4.2 Small strain stiffness anisotropy of Brno Tegel

In the hypoplastic model, stiffness anisotropy is incorporated through the tensor $\boldsymbol{\mathcal{L}}$. The general cross-anisotropic stiffness model has been presented by Mašín and Rott [22] and incorporated into

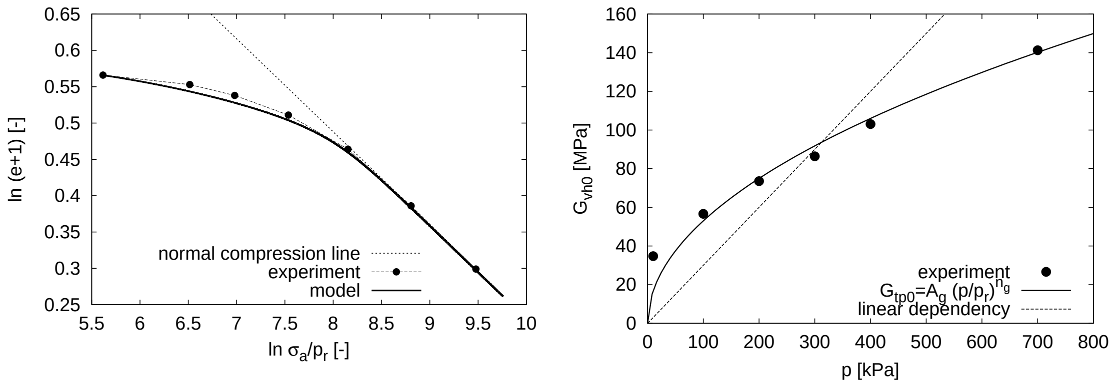

(a) (b)

Figure 6: (a) Oedometer test on undisturbed Brno Tegel sample compared with the model predictions; (b) Calibration of the model to fit the very-small-strain shear stiffness (G_{tp0}) measurements.

hypoplasticity by Mašín [21]. The model requires, in total, five further parameters: G_{tp0}, α_G, $x_{G\nu}$, x_{GE} and ν_{pp0}, where $_t$ represents direction transversal to the plane of isotropy (vertical direction) and $_p$ represents in-plane (horizontal) direction. Calibration of the very small strain shear modulus G_{tp0} has already been described above (Eq. (2)). The remaining parameters can be expressed in terms of engineering variables E_{p0}, E_{t0}, G_{pp0} and ν_{tp0} as follows [22]:

$$\alpha_G = \frac{G_{pp0}}{G_{tp0}} \tag{3}$$

$$\alpha_E = \frac{E_{p0}}{E_{t0}} = \alpha_G^{1/x_{GE}} \tag{4}$$

$$\alpha_\nu = \frac{\nu_{pp0}}{\nu_{tp0}} = \alpha_G^{1/x_{G\nu}} \tag{5}$$

Soil samples used in the investigation were obtained from the site ”Slatina”. First of all, the ratio of shear moduli α_G was investigated. Conventional bender element measurements on two pairs of soil samples were adopted: vertically trimmed samples for G_{tp0} measurements and horizontally trimmed samples (with bender elements aligned perpendicular to the bedding plane) for G_{pp0} measurements. The experiments have been performed under isotropic stress state, starting from the estimated *in-situ* mean effective stress. As demonstrated by Mašín and Rott [22], stiff to hard clays exhibit only mild effects of stress-induced anisotropy and the isotropic stress state is thus not expected to influence the results significantly. The measurement results are shown in Fig. 7a. G_{pp0} is consistently higher than G_{tp0}. For α_G quantification, the results have been approximated by a linear fit (Fig. 7a). Subsequently, the ratio α_G has been calculated from this fit as shown in Fig. 7b. The experiments indicated $\alpha_G \approx 1.45$.

To quantify the other anisotropy parameters, stress probing experiments have been performed in a

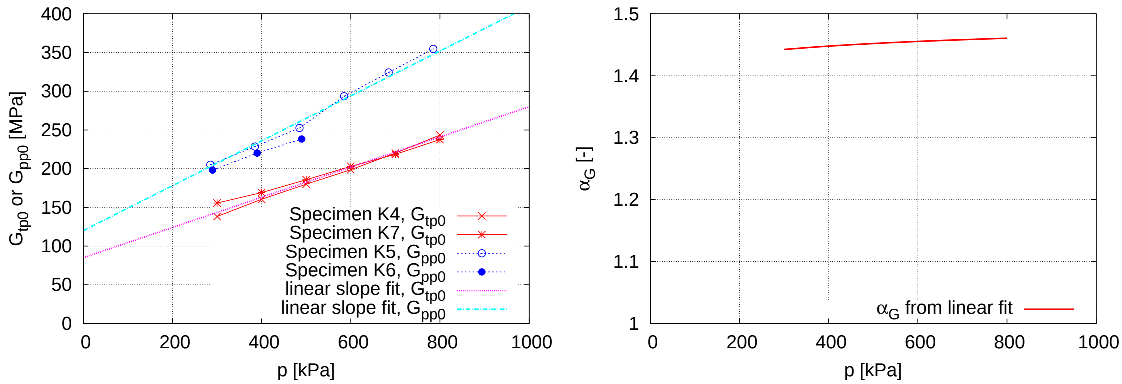

(a) (b)

Figure 7: (a) Results of bender element measurements of G_{tp0} and G_{pp0}. (b) ratio α_G calculated from the linear fit of bender element measurements.

triaxial apparatus on samples isotropically consolidated to the estimated *in-situ* mean stress state. Isotropic compression and constant radial stress stress probes on vertically trimmed samples have been performed. The samples have always been equipped with local vertical LVDT displacement transducers for axial strain ϵ_a measurements; some samples were, in addition, equipped with local LVDT transducers for radial strain ϵ_r measurement (Fig. 8). The radial strain LVDT measurements were, in addition, supplemented by ϵ_r calculated from ϵ_a measured by vertical LVDTs and conventionally measured volume strain using GDS pressure and volume controllers.

Figure 8: Setup for local LVDT measurements of radial and axial strain (LVDTs not mounted for clarity of the photograph).

The data evaluation focused on axial and radial strain measurements; comparison of statically measured moduli E_{t0} and E_{p0} and shear-wave based measurements of G_{tp0} and G_{pp0} is problematic due to the limited accuracy of LVDT measurements. Results of constant radial stress probes are in Fig. 9a. Results of local ϵ_r measurements and ϵ_r calculated from volume are consistent and indicate approximately zero radial strains. Results of the isotropic stress probes are shown in Fig. 9b. Radial strains are lower than the axial strain, which confirms the assumption about some degree of anisotropy: the measurements have been approximated by a linear fit $\epsilon_r = 0.6\epsilon_a$.

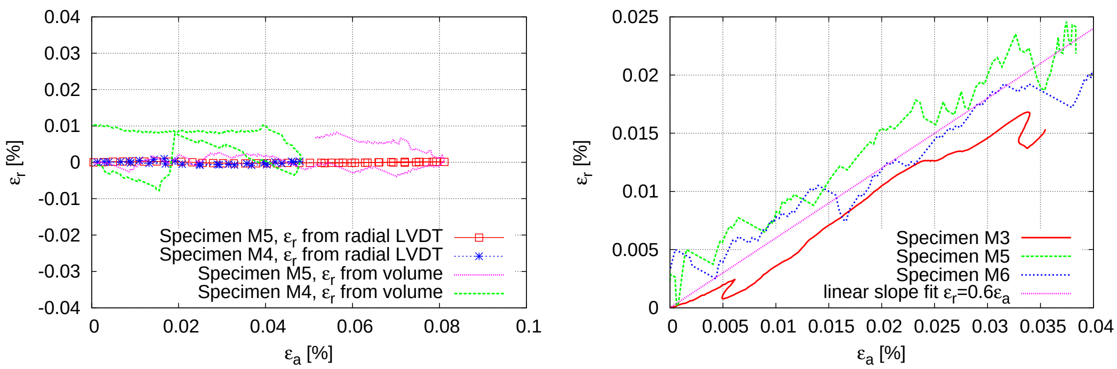

(a) (b)

Figure 9: (a) ϵ_r vs. ϵ_a measured in constant radial stress probes; (b) ϵ_r vs. ϵ_a measured in isotropic stress probes (specimen M3: local LVDT ϵ_r measurement; specimens M5 and M6: ϵ_r calculated from volume).

The stress probing experiments can be evaluated using transversely isotropic compliance matrix. The shear components of stress and strain tensors are zero in the experiment in the triaxial apparatus, so

$$\begin{bmatrix} \dot{\epsilon}_a \\ \dot{\epsilon}_r \\ \dot{\epsilon}_r \end{bmatrix} = \begin{bmatrix} \frac{1}{E_{t0}} & -\frac{\nu_{pt0}}{E_{p0}} & -\frac{\nu_{pt0}}{E_{p0}} \\ -\frac{\nu_{tp0}}{E_{t0}} & \frac{1}{E_{p0}} & -\frac{\nu_{pp0}}{E_{p0}} \\ -\frac{\nu_{tp0}}{E_{t0}} & -\frac{\nu_{pp0}}{E_{p0}} & \frac{1}{E_{p0}} \end{bmatrix} \begin{bmatrix} \dot{\sigma}_a \\ \dot{\sigma}_r \\ \dot{\sigma}_r \end{bmatrix} \tag{6}$$

where the subscript $_t$ represents direction transversal to the plane of isotropy (vertical direction) and the subscript $_p$ represents in-plane (horizontal) direction. It follows from (6) that for constant radial stress probes with $\dot{\sigma}_r = 0$ the ratio of radial and axial strains (in-plane and transversal strains for the vertically trimmed sample) is given by

$$\frac{\dot{\epsilon}_r}{\dot{\epsilon}_a} = -\nu_{tp0} \tag{7}$$

Negligible radial strains measured in the experiment (Fig. 9a) thus imply $\nu_{tp0} \approx 0$.

The strain ratio $\dot{\epsilon}_r/\dot{\epsilon}_a$ of the isotropic compression test ($\dot{\sigma}_t = \dot{\sigma}_p$) can be calculated from:

$$\frac{\dot{\epsilon}_r}{\dot{\epsilon}_a} = \frac{-\nu_{tp0} + \frac{1}{\alpha_E} - \frac{\alpha_\nu}{\alpha_E}\nu_{tp0}}{1 - 2\nu_{tp0}} \tag{8}$$

By considering $\nu_{tp0} \approx 0$ obtained from the evaluation of the constant radial stress probes, Eq. (8) simplifies to

$$\frac{\dot{\epsilon}_r}{\dot{\epsilon}_a} = \frac{1}{\alpha_E} \tag{9}$$

The experimentally obtained $\dot{\epsilon}_r/\dot{\epsilon}_a = 0.6$ thus implies $\alpha_E \approx 1.67$. Combining this value of α_E with $\alpha_G \approx 1.45$ obtained from bender element measurements imply $x_{GE} \approx 0.73$. This value is close to $x_{GE} = 0.8$, suggested by Mašín and Rott [22] on the basis of experimental database from the literature.

The available data do not allow us to quantify ν_{pp0} and α_ν, Mašín and Rott [22] was thus followed, who suggested $\alpha_\nu = \alpha_G$ and assume $\nu_{pp0} = \nu_{tp0} = 0$. It is to be pointed out that for our case with $\nu_{tp0} = 0$, α_ν is undefined and assumption $\nu_{pp0} = \nu_{tp0}$ is not supported by any physical reason. However, a parametric study using Eq. (8) reveals that the assumed value of ν_{pp0} has little influence on the obtained value of α_E. Subsequently, it was also demonstrated that this assumption has a minor effect on the back-calculated value of K_0. Note also, that in hypoplasticity the parameter ν is adopted to control large-strain stiffness, and it is not possible to set ν independently for the very-small-strain ragion. ν value from Tab. 1 was thus adopted, while it was checked that the actual value of this parameter does not substantially affect the predictions.

The small strain stiffness anisotropy parameters are summarised in Tab. 2.

Table 2: *Small strain stiffness anisotropy coefficients of the Brno Tegel*

α_G	x_{GE}	ν_{tp0}	$x_{G\nu}$
1.45	0.73	0	(1)

4.3 Strata overlying Brno Tegel

The geological sequence consists, in addition to Brno Tegel, of the overlying loess loams, clayey loams and sandy gravels. Svoboda et al. [34] studied the influence of material properties of these geological layers on predictions of surface displacements due to tunnelling, and found that their influence is minor. For this reason, these layers were out of focus of this study and they were simulated using the basic Mohr-Coulomb constitutive model with parameters summarised in Tab. 3.

Table 3: *Mohr-Coulomb model parameters of the layers overlying the Brno Tegel strata.*

soil	φ [°]	c [MPa]	ψ [°]	E [MPa]	ν	γ [kN/m^3]
backfill	20	10	4	10	0.35	19
loess loam	28	2	2	45	0.4	19
clayey loam	15	18	2	50	0.4	20
sand with gravel	30	5	8	60	0.35	19

4.4 Tunnel lining description

The circular exploratory cavity has been unsupported. However, support has been used in the main triangular exploratory adit (Fig. 4a) and, obviously, in the main tunnel. The dependency of their stiffness on time had to be specified. The primary lining has been composed of two components: shotcrete and massive steel supports. Shotcrete was used in two layers 0.175 m each for the main tunnel and one 0.1 m layer for the exploratory adit. Steel support HEB 240 (H-profile steel beam 240 mm x 240 mm) has been adopted in the main tunnel, whereas U-shaped rolled steel beam mining support K24 (width 125 mm, height 107 mm) was used in the exploratory adit. The lining has been modelled using shell elements characterised by a single parameter set obtained using homogenisation procedure proposed by Rott [29]. The dependency of Young modulus and bending stiffness on time for the triangular exploratory adit and for the main tunnel obtained from the homogenisation procedure is shown in Fig. 10; detailed description of the procedure is outside the scope of the present paper and the readers are referred to [29]. As the adopted software did not allow for time-dependent shotcrete parameters, the parameters were manually adjusted after each calculation phase.

5 Description of finite element models

Two 3D finite element models have been set up in the software Plaxis 3D. The first model represented the triangular exploratory adit with the cylindrical cavity side-drift, the second model represented the complete Královo Pole tunnel. In the following, two models are described. Both the models adopted unstructured finite element meshes composed of 10-node tetrahedral elements with a second-order interpolation of displacements. The excavation process was simulated as undrained using penalty approach [28, 4]. The adopted values of bulk modulus of water were $K_w = 2.1$ GPa.

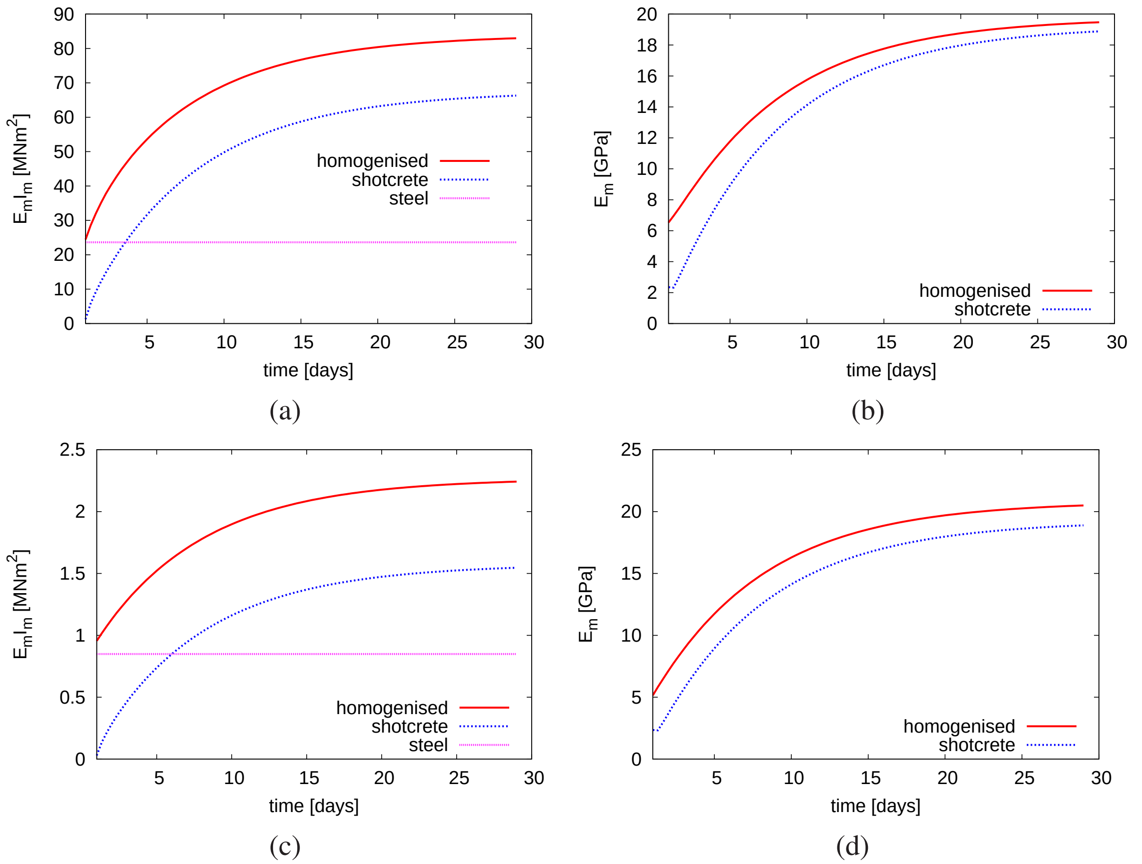

Figure 10: The dependency of lining bending stiffness (a,c) and Young modulus (b,d) for the main tunnel (a,b) and the triangular exploratory adit (c,d).

5.1 Model of the triangular exploratory adit and the unsupported cylindrical cavity

As the stress state in the soil massif is influenced by the preceding excavation of the triangular exploratory adit, cylindrical cavity excavation had always to be simulated together with the triangular exploratory gallery excavation. The modelled section of the triangular exploratory gallery was 18 m long. Model consisted of 36000 tetrahedral elements, its geometry may be seen in Fig. 11. The complete numerical analysis was composed of 28 phases and each of the phases represented the progress of the excavation of 1.2 m (except the portion containing junction, see Fig. 11). The overburden was 22.1 m above the crown of the unsupported cylindrical cavity (20.4 m above the crown of the triangular exploratory gallery). Excavation of the modelled portion of the exploratory gallery and unsupported cylindrical cavity were fast (they took 6 days in total), and therefore the analyses were undrained. Ground water table coincided with the top of the Brno Tegel layer and soil below the ground water table we considered as fully saturated.

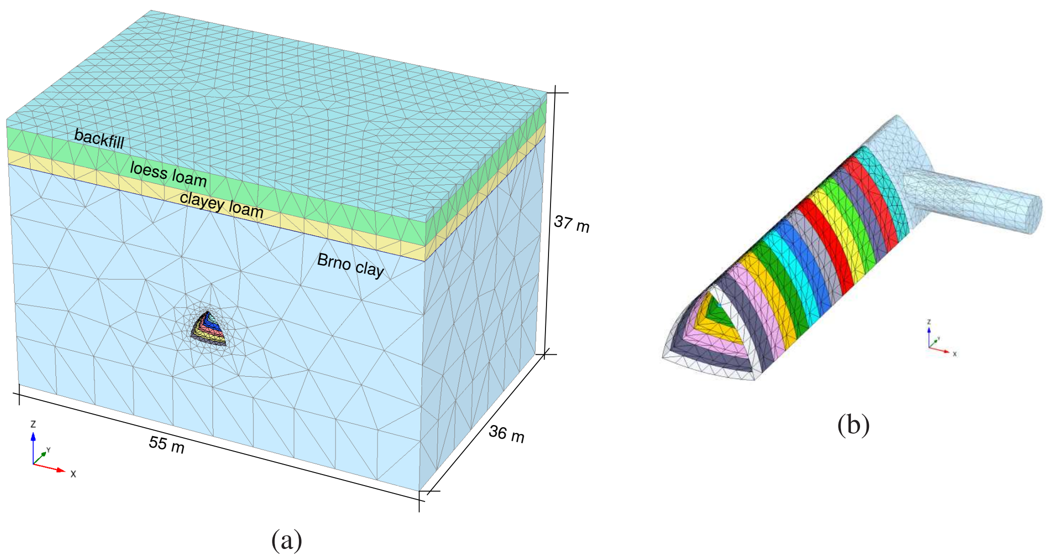

Figure 11: A complete finite element model and the mesh of the triangular exploratory gallery and cylindrical cavity (a); detail of the excavations (b).

5.2 Model of the Královo Pole tunnel

To further verify the back-analysed value of K_0, a finite element model of the complete Královo Pole tunnel has been set up. The same tunnel has already been simulated by Svoboda et al. [34], who presented class A predictions of its excavation. They obtained good agreement between the monitored and simulated surface settlement troughs. However, horizontal deformations measured by inclinometers have been overestimated. Svoboda et al. [34] attributed it to improper characterisation of soil stiffness anisotropy. In this paper, a soil constitutive model capable of predicting stiffness anisotropy and a more detailed model for the lining stiffness evolution with time were adopted. In addition, different tunnel section was selected (closer to the simulated cylindrical cavity). The simulated section was within a sparsely built-up area, without any compensation grouting or micropile umbrella applied and without the exploratory adit, which simplified the model setup and introduced less ambiguity into the comparison with monitoring data.

The finite element model was composed of 31000 tetrahedral elements. The simulated portion was 56.4 metres long and corresponded to the tunnel chainage 0.651 - 0.707 km. This section was not affected by any geometry complexities (such as widening and safety bays) or by sub-surface compensation grouting. The results from numerical analysis were compared with monitoring data from the inclinometer in km 0.675 and from the geodetically measured surface settlement trough in km 0.740. The overburden was 17.2 m. The ground water table was considered to coincide with the top of Brno Tegel, the soil below the water table was treated as fully saturated. The numerical analysis was composed of 76 phases; each phase represented progress of excavation by 1.2 m and it was excavated within the period of 8 hours. The excavation order has been described in Sec. 3 (Fig. 3). The first 1.2 m of excavation remained always unsupported, the lining stiffness then increased with time. The complete model geometry is shown in Fig. 12a, detailed view of the tunnel in Fig. 12b.

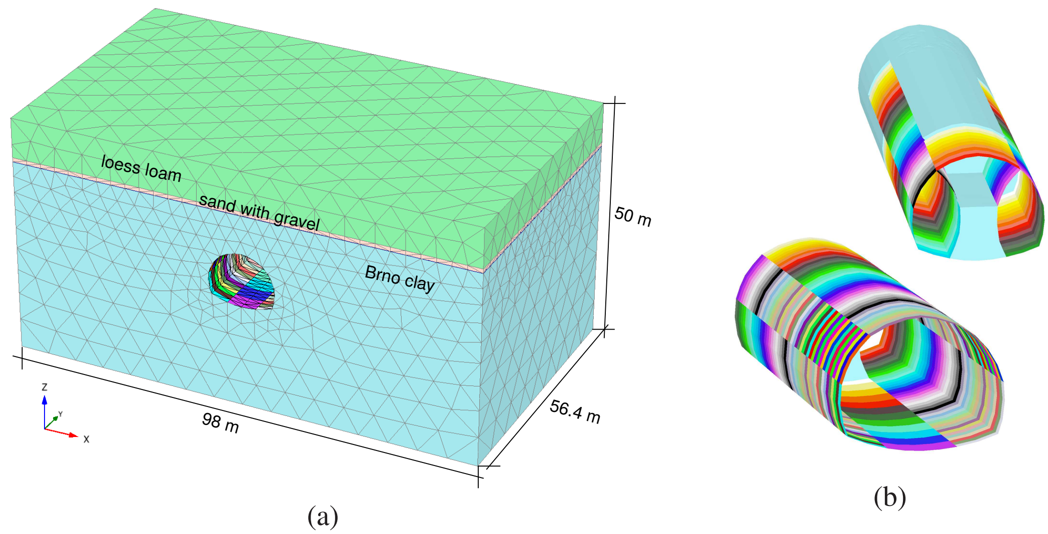

Figure 12: (a) A complete finite element model and the mesh of the Královo Pole tunnel; (b) detail of the tunnel showing the excavation steps; complete tunnel (bottom) and partial state at the time of the inclinometric measurements (top).

6 Back-analyses of K_0 using the cylindrical cavity simulations

The procedure of the back-analyses was as follows. K_0 is influencing the horizontal stress (not affecting the vertical stress), and it is thus a factor affecting the ratio of horizontal u_h and vertical u_v convergences of the cylindrical cavity. In the analyses, K_0 was varied until the model predicted the measured ratio $u_h/u_v = 1.248$. In the evaluation, pre-convergence was taken into account. That is, u_h and u_v represented the difference between the values at the time of measurement and the values at the time of the convergence mark installation, rather than the total displacements of soil. In all the back-analyses, simulating the complete triangular gallery preceded simulations of cylindrical cavity. The calculated distribution of (total) vertical and horizontal displacements around the cylindrical cavity for the parameters from Sec. 4 and $K_0 = 0.81$ is in Fig. 13.

Figure 14a shows the dependency of the ratio u_h/u_v on the value of K_0 for $\alpha_G = 1.35$ and parameters[2] from Tab. 1. Clearly, K_0 influences the calculated ratio u_h/u_v quite remarkably. As

[2] $\alpha_G = 1.35$ was a preliminary experimental estimate of α_G, more detailed experimental study has later indicated $\alpha_G = 1.45$.

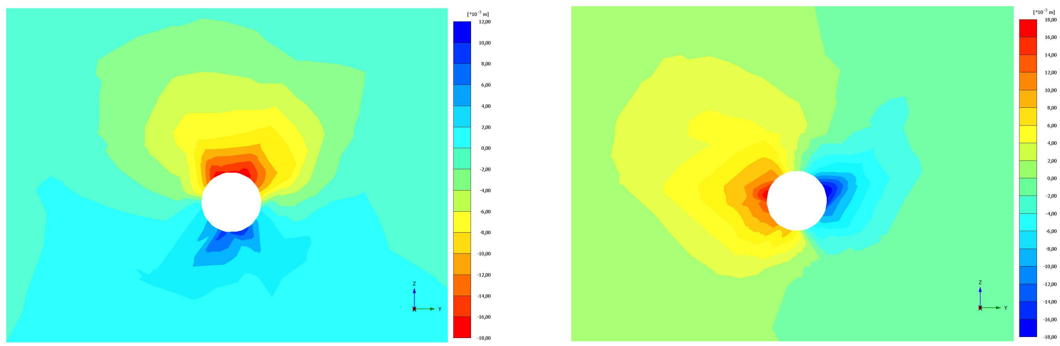

(a) (b)

Figure 13: Predicted total displacements around the cylindrical cavity for the parameters from Sec. 4 and $K_0 = 0.81$. (a) vertical displacements u_v, (b) horizontal displacements u_h.

expected, increasing K_0 increases the ratio u_h/u_v but, interestingly, it is the value of u_v and not u_h which is influenced the most by K_0 (Fig. 14b).

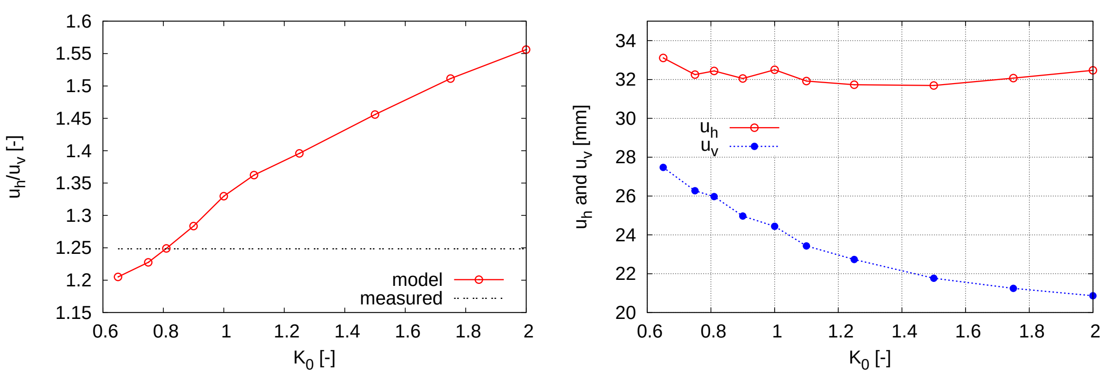

(a) (b)

Figure 14: The influence of the ratio u_h/u_v (a) and the values of u_v and u_h (b) of the cylindrical cavity on K_0 for $\alpha_G = 1.35$.

To investigate the effect of uncertainty in the value of α_G, the back-analyses were performed with several α_G values. The dependency of the back-analysed K_0 on the value of α_G is in Fig. 15. An increase in α_G decreases the back-calculated value of K_0. For $\alpha_G = 1.45$ the model implies $K_0 = 0.75$. This value is close to normally consolidated conditions: Jáky [13] formula yields $K_0 = 1 - \sin\varphi_c = 0.63$ for $\varphi_c = 22°$. The OCR-based estimation follows formula by Mayne and Kulhawy [23]

$$K_0 = (1 - \sin\varphi_c)\, OCR^{\sin\varphi_c} \tag{10}$$

The vertical preconsolidation pressure of Brno Tegel is approx. 1800 kPa (measured in [34]) and the vertical effective stress in the cavity depth is approx. 260 kPa, and thus $OCR \approx 7$. These values imply $K_0 = 1.3$.

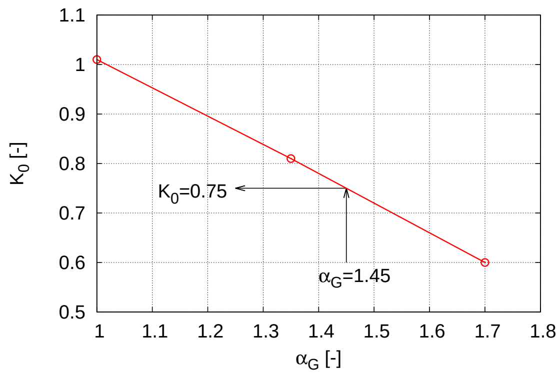

Figure 15: The influence of the α_G on the back-calculated value of K_0.

In the subsequent parametric analyses, sensitivity of the results to different parameters was investigated. The influence of α_G, x_{GE} and $x_{G\nu}$ on the value of the ratio u_h/u_v is shown in Fig. 16 ($K_0 = 0.81$ is adopted, the initial values of $\alpha_G = 1.35$, $x_{GE} = 0.8$ and $x_{G\nu} = 1$ are used and only one parameter is varied at a time). While the effect of α_G on the calculated u_h/u_v is quite substantial, the influence of x_{GE} and $x_{G\nu}$ is much less significant.

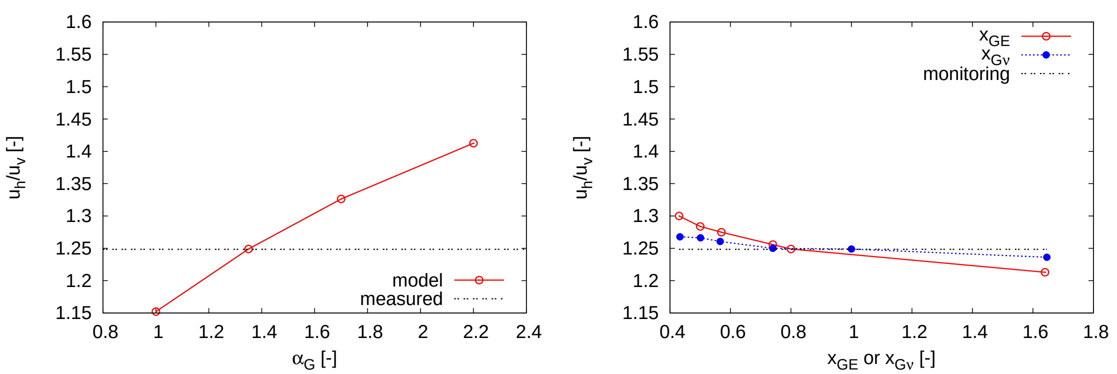

(a) (b)

Figure 16: The influence of α_G (a) and x_{GE} and $x_{G\nu}$ (b) on the ratio u_h/u_v for $K_0 = 0.81$.

It is to be pointed out that the positive dependency of the predicted u_h/u_v on α_G is counter-intuitive. It would be expected that an increase of the horizontal stiffness at a constant vertical stiffness (increase of α_G with constant A_g and n_g) would decrease the horizontal displacements and thus also the ratio u_h/u_v. The positive dependency of u_h/u_v on α_G is caused by the undrained conditions; anisotropy affects not only the stiffness (which is higher in horizontal direction in anisotropic soil), but also the undrained stress path (higher excess pore water pressures are generated while shearing the anisotropic soil). Very small strain stiffness depends not only on anisotropy but also on mean effective stress. Consequently, stiffness decrease due to lower mean effective stress may outperform horisontal stiffness increase due to soil anisotropy, leading finally to a positive dependency of u_h/u_v on α_G shown in Fig. 16a.

7 Verification by simulating the triangular adit and Královo Pole tunnel

Different sets of monitoring data are available for both the triangular exploratory gallery and for the main Královo Pole tunnel. In particular, geodetic data are available for the surface settlement troughs and inclinometric measurements are available quantifying horizontal displacements in the vicinity of the tunnels. In addition, convergence measurements and lining tangential stress measurements (using tensiometers) have been performed in the exploratory gallery and geodetic measurements of lining deformations have been performed in the main tunnel.

In Fig. 17a, surface settlement trough of the main Královo Pole tunnel is compared with predictions for different combinations of α_G and K_0, which led to the same ratio $u_h/u_v = 1.248$ in the cylindrical cavity simulations. Several monitoring data sets are included in Fig. 17a, all in a near distance to the modelled section and with similar geological profile. The section exactly corresponding to the modelled one is denoted as ”km 0.740”. The simulations represent the monitoring data well, while there is only a little influence of the α_G-K_0 combination. Similar relatively accurate predictions of the surface settlement trough have been achieved by Svoboda et al. [34] in their Class A predictions of Královo Pole tunnel excavation. Svoboda et al. [34], however, significantly overestimated horizontal displacements measured by inclinometers. Those are represented relatively accurately by the present model (Fig. 17b), with the combination $K_0 = 0.6$ vs. $\alpha_G = 1.7$ leading to the best predictions. It is pointed out that while the different α_G-K_0 combinations led to the same predictions of u_h/u_v ratio in the unsupported cylindrical cavity, they lead to different predictions in the case of the main tunnel. Decrease of K_0 accompanied by the increase of α_G leads to a decrease of horizontal displacements, as would intuitively be expected.

Results of geodetic measurements of an evolution of tunnel lining deformation with time are shown in Fig. 18. In evaluating the results, pre-convergences were subtracted from the total displacements. The fit is obviously not exact, the model however predicted reasonably well both the displacement magnitude and its time evolution.

Figure 19 shows measured and simulated ground surface settlements and horizontal displacements in inclinometers of the triangular exploratory adit. The comparisoan of simulations and measurements is, in general, similar to the main tunnel. In this case, the used combinations α_G-K_0 led to

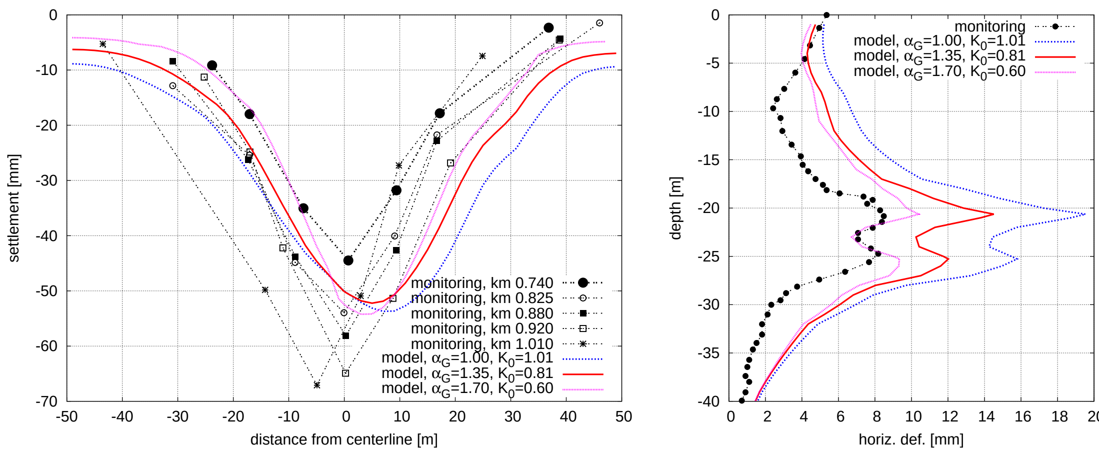

(a) (b)

Figure 17: Surface settlement trough (a) and horizontal displacements (b) of the main Královo Pole tunnel predicted by the models with different combinations of α_G - K_0 compared with monitoring data.

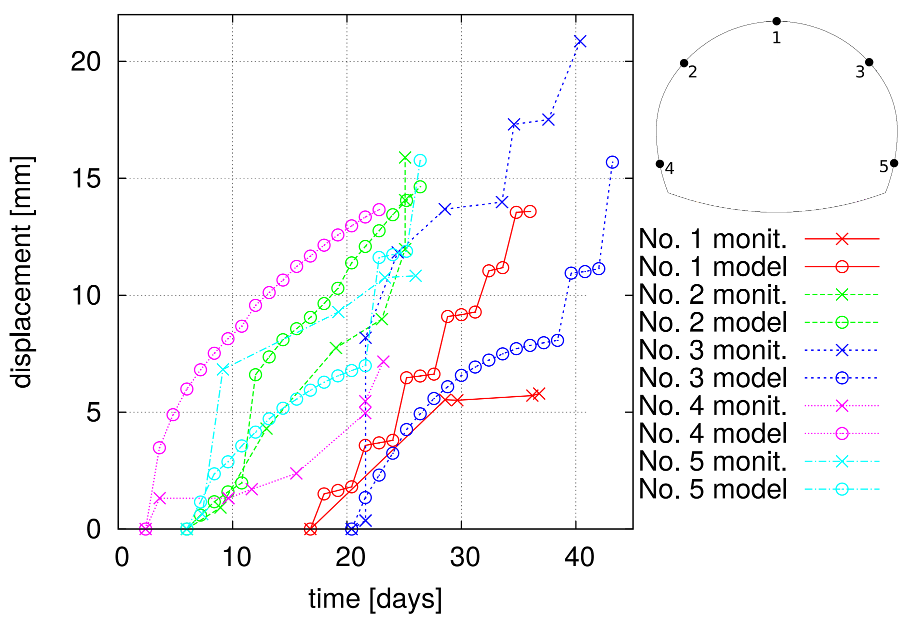

Figure 18: A graph showing time-evolution of monitored and calculated magnitude of lining displacements in five different locations along the tunnel.

a slightly more significant influence on the surface settlement trough shape and depth, and smaller influence on the horizontal displacements. For all α_G-K_0 combinations the predictions are reasonable, $K_0 = 0.6$ vs. $\alpha_G = 1.7$ combination leading to the best predictions in terms of horizontal displacement, but overestimating settlement trough depth.

Convergence measurements in three profiles inside the triangular exploratory adit are in Fig. 20.

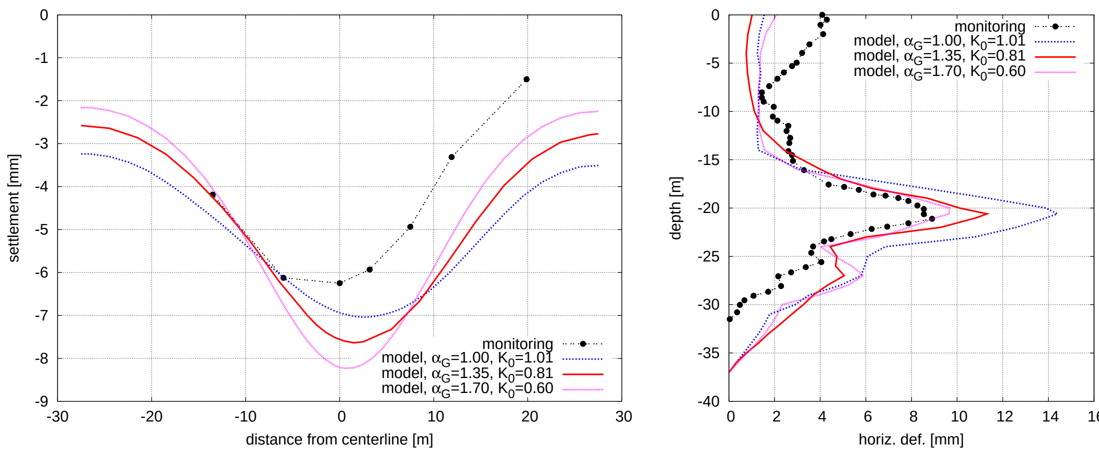

(a) (b)

Figure 19: Surface settlement trough (a) and horizontal displacements (b) of the triangular exploratory adit predicted by the models with different combinations of α_G - K_0 compared with monitoring data.

Fig. 20a shows the monitoring scheme and Fig. 20b shows the development of displacements with time. The analyses were performed as undrained, so the soil response is not time-dependent, however the dependence of convergence on time is still predicted thanks to the three-dimensional effects in the simulation (adit face progress) and time-dependence of the lining stiffness. The convergence rate is overpredicted, nevertheless the final values are predicted reasonably well.

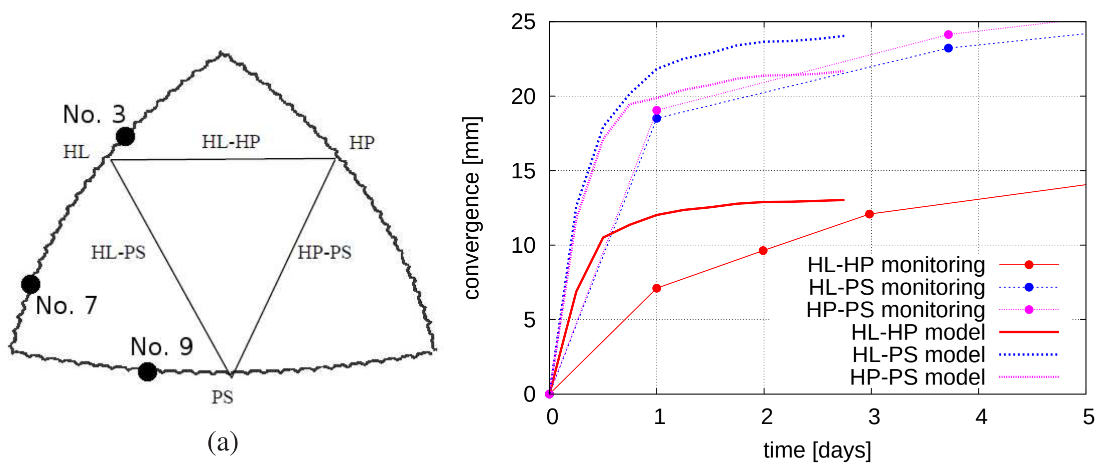

(a) (b)

Figure 20: (a) The triangular adit convergence monitoring scheme (including location of lining tangential stress measurements), (b) comparison of monitoring results with simulations with $K_0 = 0.81$ and $\alpha_G = 1.35$.

Development of tangential stress in the primary lining of the exploratory adits are shown in Fig. 21.

The stresses were estimated from tensiometer measurements. Stresses in location No. 7 (position on measurements points is in Fig. 20) are predicted reasonably well. Much lower values have been measured in locations No. 3 and No. 9. It is not possible to decisively conclude whether the simulation results are incorrect or whether the discrepancy is caused by a malfunction of the measurement device.

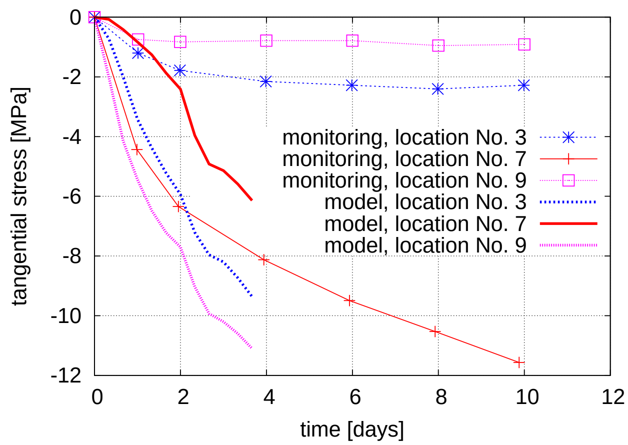

Figure 21: Development of tangential stress in the primary lining of exploratory adits with time, starting at the beginning of the excavation: monitoring data and the model.

8 Conclusions

In the paper, coefficient of earth pressure at rest K_0 in stiff to hard clay was investigated by means of back-analysis of monitoring results from unsupported cylindrical cavity. The results have been verified by analysing the triangular exploratory gallery and the road tunnel. To this aim, cross-anisotropic characteristics of Brno Tegel were studied; in particular the ratio of horizontal and vertical shear moduli was measured as $\alpha_G = G_{pp0}/G_{tp0} = 1.45$, the ratio of horizontal and vertical Young moduli as $\alpha_E = E_{p0}/E_{t0} = 1.67$ and the value of vertical Poisson ratio as $\nu_{tp0} = 0$. Such detailed measurements of clay anisotropy are not common in the geotechnical literature.

The value of $K_0 = 0.75$ was found by back-analysis. This value is remarkably low, considering the clay is of stiff to hard consistency with apparent vertical preconsolidation pressure of 1.8 MPa and apparent OCR in the tunnel depth of OCR$\approx$ 7. Jáky's [13] formula in this case yields $K_0 = 0.63$, while an estimation based on apparent preconsolidation from the formula of Mayne and Kulhawy [23] implies $K_0 = 1.3$. Notwithstanding the complexity of the analysis a number of uncertainties, the K_0 value was relatively close to the K_0 of normally consolidated soil. This would indicate that a significant portion of the apparent overconsolidation of Brno clay was caused by the effects of ageing. Detailed discussion of Brno clay geological history is, however, outside the scope of the present paper and it is planned to be covered in the future work.

Our conclusions obviously cannot be generalised to all stiff clays, as the K_0 value of any soil depends on its unique geological history. It controls the relative influence of ageing (the secondary compression in particular) and mechanical unloading due to erosion on the preconsolidation pressure. It can, however, be concluded that OCR-based formulas should not be used automatically for K_0 estimation, as they may potentially lead to a significant K_0 overestimation.

9 Acknowledgment

Financial support by the research grants 15-05935S, 14-32105S and P105/12/1705 of the Czech Science Foundation and by the research grant No. GAUK 243-253370 of the Charles University Grant Agency is greatly appreciated.

References

[1] J. Bača and V. Dohnálek. Královo Pole tunnels - experience obtained during the construction to date. *Tunel*, 18(3):27–32, 2009.

[2] L. Bjerrum and K. Andersen. In-situ measurement of lateral pressures in clay. In *Proc.* 5^{th} *European Conference on Soil Mechanics and Geotechnical Engineering, Madrid*, volume 1, pages 12–20, 1972.

[3] J. Boháč, D. Mašín, R. Malát, V. Novák, and J. Rott. Methods of determination of K_0 in overconsolidated clay. In P. Delage, J. Desrues, R. Frank, A. Puech, and F. Schlosser, editors, *Proceedings of the 18th International Conference on Soil Mechanics and Geotechnical Engineering*, volume 1, pages 203–206, 2013.

[4] R. I. Borja. Analysis of incremental excavation based on critical state theory. *Journal of Geotechnical Engineering ASCE*, 116(6):964–985, 1990.

[5] J. B. Burland and J. Maswoswe. Discussion on "In situ measurements of horizontal stress in overconsolidated clay using push-in spade-shaped pressure cells". *Géotechnique*, 32(2):285–286, 1982.

[6] M. Doležalová. Approaches to numerical modelling of ground movements due to shallow tunnelling. In *Proc.* 2^{nd} *Int. Conference on Soil Structure Interaction in Urban Civil Engineering, ETH Zürich*, pages 365–376, 2002.

[7] I. Doran, V. Sivakumar, J. Graham, and A. Johnson. Estimation of in situ stresses using anisotropic elasticity and suction measurements. *Géotechnique*, 50(2):189–196, 2000.

[8] J. N. Franzius, D. M. Potts, T. I. Addenbrooke, and J. B. Burland. The influence of building weight on tunnelling-induced ground and building deformation. *Soils and Foundations*, 44(1):25–38, 2005.

[9] G. Gudehus. A comprehensive constitutive equation for granular materials. *Soils and Foundations*, 36(1):1–12, 1996.

[10] G. Gudehus and D. Mašín. Graphical representation of constitutive equations. *Géotechnique*, 59(2):147–151, 2009.

[11] K. Hamouche, S. Leroueil, M. Roy, and A. J. Lutenegger. In situ evaluation of k0 in eastern canada clays. *Canadian Geotechnical Journal*, 32(4):677–688, 1995.

[12] V. Horák. Kralovo pole tunnel in Brno from designer point of view. *Tunel*, 18(1):67–72, 2009.

[13] J. Jáky. The coefficient of earth pressure at rest. *Journal for Society of Hungarian Architects and Engineers*, pages 355–357, 1944.

[14] E. Kavazanjian and J. K. Mitchell. Time dependence of lateral earth pressure. *Journal of Geotechnical Engineering ASCE*, 110(4):530–533, 1984.

[15] G. Lefebvre, M. Bozozuk, A. Philibert, and P. Hornych. Evaluating k0 in champlain clays with hydraulic fracture tests. *Canadian Geotechnical Journal*, 28(3):365–377, 1991.

[16] S. Marchetti. In situ tests by flat dilatometer. *Journal of Geotechnical Engineering Division ASCE*, 106(NoGT3):299–321, 1980.

[17] D. Mašín. A hypoplastic constitutive model for clays. *International Journal for Numerical and Analytical Methods in Geomechanics*, 29(4):311–336, 2005.

[18] D. Mašín. Asymptotic behaviour of granular materials. *Granular Matter*, 14(6):759–774, 2012.

[19] D. Mašín. Hypoplastic Cam-clay model. *Géotechnique*, 62(6):549–553, 2012.

[20] D. Mašín. Clay hypoplasticity with explicitly defined asymptotic states. *Acta Geotechnica*, 8(5):481–496, 2013.

[21] D. Mašín. Clay hypoplasticity model including stiffness anisotropy. *Géotechnique*, 64(3):232–238, 2014.

[22] D. Mašín and J. Rott. Small strain stiffness anisotropy of natural sedimentary clays: review and a model. *Acta Geotechnica*, 9(2):299–312, 2014.

[23] P. W. Mayne and F. H. Kulhawy. K_0–OCR relationships in soil. In *Proc. ASCE J. Geotech. Eng. Div.*, volume 108, pages 851–872, 1982.

[24] G. Mesri and A. Castro. C_α/C_c concept and K_0 during secondary compression. *Journal of Geotechnical Engineering ASCE*, 113(3):230–247, 1987.

[25] G. Mesri and T. M. Hayatt. The coefficient of earth pressure at rest. *Canadian Geotechnical Journal*, 30:647–666, 1993.

[26] A. Niemunis and I. Herle. Hypoplastic model for cohesionless soils with elastic strain range. *Mechanics of Cohesive-Frictional Materials*, 2(4):279–299, 1997.

[27] J. Pavlík, L. Klímek, and D. Rupp. Geotechnical exploration for the Dobrovského tunnel, the most significant structure on the large city ring road in Brno. *Tunel*, 13(2):2–12, 2004.

[28] D. M. Potts and L. Zdravkovic. *Finite element analysis in geotechnical engineering. Volume I: Theory*. Thomas Telford, London, 1999.

[29] J. Rott. Homogenisation and modification of composite steel-concrete lining, with the modulus of elasticity of sprayed concrete growing with time. *Tunel (www.ita-aites.cz/en/casopis)*, 23(3):53–60, 2014.

[30] J. H. Schmertmann. A simple question about consolidation. *Journal of Geotechnical Engineering ASCE*, 109(1):119–122, 1983.

[31] A. W. Skempton. Horizontal stresses in an over-consolidated eocene clay. In *Proc.* 5^{th} *Int. Conf. Soil Mechanics and Foundation Engineering*, volume 1, pages 351–357, 1961.

[32] T. Svoboda and D. Mašín. Comparison of displacement fields predicted by 2D and 3D finite element modelling of shallow NATM tunnels in clays. *Geotechnik*, 34(2):115–126, 2011.

[33] T. Svoboda, D. Mašín, and J. Boháč. Hypoplastic and mohr-coulomb models in simulations of a tunnel in clay. *Tunel*, 18(4):59–68, 2009.

[34] T. Svoboda, D. Mašín, and J. Boháč. Class A predictions of a NATM tunnel in stiff clay. *Computers and Geotechnics*, 37(6):817–825, 2010.

[35] P. Tedd and J. A. Charles. In situ measurements of horizontal stress in overconsolidated clay using push-in spade-shaped pressure cells. *Géotechnique*, 31(4):554–558, 1981.

[36] C. Wroth and J. Hughes. An instrument for the in-situ measurements of the properties of soft clays. In *Proc.* 8^{th} *Int. Conference on Soil Mechanics and Foundation Engineering, Moscow*, volume 1, pages 487–494, 1973.

[37] I. Zemánek, J. Lossmann, and K. Socha. Impact of exploration galleries for the Dobrovského tunnel on surface development in Brno; application of the observation method. *Tunel*, 12(3):33–37, 2003.